ATP-Dependent Structural Changes of the Outer Dynein Arm in *Tetrahymena* Cilia: A Freeze-etch Replica Study

SHOICHIRO TSUKITA, SACHIKO TSUKITA, JIRO USUKURA, and HARUNORI ISHIKAWA
Department of Anatomy, Faculty of Medicine, University of Tokyo, Hongo 7-3-1, Bunkyo-ku, Tokyo 113, Japan

ABSTRACT With the rapid-freeze, deep-etch replica technique, the structural conformations of outer dynein arms in demembranated cilia from *Tetrahymena* were analyzed under two different conditions, i.e., in the absence of ATP and in the presence of ATP and vanadate. In the absence of ATP, the lateral view of axonemes was characterized by the egg-shaped outer dynein arms, which showed a slightly baseward tilt with a mean inclination of 11.1° ± 3.4° SD from the perpendicular to the doublet microtubules. On the other hand, in the presence of 1 mM ATP and 100 μM vanadate, the outer arms were extended and slender and showed an increased baseward tilt with a mean inclination of 31.6° ± 4.9° SD. In ATP-activated axonemes, these two types of arms coexisted, each type occurring in groups along one row of outer arms. These findings strongly suggest that the interdoublet sliding is caused by dynamic structural changes of dynein arms that follow the hydrolysis of ATP.

Since Satir (1) first obtained evidence for the sliding tubule hypothesis for ciliary movement from electron microscopic observations, and Summers and Gibbons (2) successfully demonstrated that ATP-induced active sliding of adjacent doublet microtubules in trypsin-treated, demembranated axoneme preparations, isolated axonemes have been used as a highly advantageous model for mechanochemical analysis of cilia and flagella. It is now widely accepted that the two rows of dynein arms on the A-tubule of each doublet are responsible for ATP-induced active sliding in axonemes. Although the broad outlines of this sliding-tubule model appear to have been well established, there is at present very little data to explain at the molecular level how dynein arms convert the chemical energy of ATP into the mechanical work for interdoublet sliding (3).

By analogy with myosin in striated muscle, the mechanochemical cycle of dynein arms may comprise the following processes: (*a*) the formation of cross-bridges of dynein arms between adjacent doublets, (*b*) the structural changes of the dynein arms, and (*c*) the detachment of the dynein arms from B-tubules of the doublets (4, 5). At present, however, our knowledge of the structural changes of the dynein arms is still limited. Sale and Satir (6) first demonstrated the baseward tilt of the dynein arms on the A-tubules of isolated axonemes. Warner and Mitchell (7) further substantiated the baseward tilt of dynein arms in both the "bridged" and "unbridged" states. Recently, Takahashi and Tonomura (8) elegantly showed that 30S dynein from *Tetrahymena* cilia bound to both the A- and B-tubules of isolated doublets with a baseward tilt and that ATP caused dissociation of the dynein from the B-tubule. They suggested that in the presence of ATP the dynein arms might undergo an attachment-detachment cycle with changes in their tilting angle. All these results were obtained by negative-stain electron microscopy of disintegrated axonemes of *Tetrahymena* cilia. Unfortunately, in negative staining, it is not easy to control the physiological environment of the dynein arms with respect to free Mg^{++}, ATP, ADP, etc. Furthermore, in negatively stained preparations, the possible superimposition effect of outer and inner dynein arms (and the spoke structures, in some cases) may obscure the images of individual dynein arms.

The freeze-etch replica technique combined with rapid freezing has been successfully applied to ultrastructural analyses of many cellular processes (9–12). This technique can provide information about the three-dimensional organization of structures at high resolution without chemical fixation. Furthermore, the "temporal resolution" can be expected to be 2 ms or better in rapid freezing using liquid helium (9). Hence, we have used this technique to analyze the structural changes of dynein arms in axonemes during the mechanochemical cycle. This paper describes (*a*) the structural differences between outer dynein arms in the absence of ATP and in the presence of ATP and vanadate, a specific dynein ATPase inhibitor (13), and (*b*) the structural changes of outer arms during the ATP-hydrolysis cycle. In this study, to avoid specimen deformation, frozen samples were not fractured. Therefore, our observations were limited to the lateral view of isolated axonemes.

MATERIALS AND METHODS

Isolation of Cilia: *Tetrahymena pyriformis*, strain W, was grown in 2% proteose peptone, 1% glucose, and 0.2% yeast extract (pH 7.3) at 27°C. After 4 d in culture, the cells were harvested by gentle centrifugation (400 *g*). The cilia were isolated according to the ethanol-calcium procedure used by Takahashi and Tonomura (8), a modification of the original method of Watson and Hopkins

THE JOURNAL OF CELL BIOLOGY · VOLUME 96 MAY 1983 1480-1485

(14) and Gibbons (15). All subsequent preparative steps were carried out at 4°C unless otherwise stated. Isolated cilia were suspended in 25 mM KCl, 2.5 mM $MgSO_4$, 0.2 M sucrose, 1 mM dithiothreitol (DTT), and 30 mM Tris-thioglycolate buffer (pH 8.3) and mixed with an equal volume of the same buffer solution containing 1% (vol/vol) Triton X-100. After an 8-min incubation, the demembranated axonemes were centrifuged at 12,000 *g* for 20 min, and the axonemal pellet was gently resuspended in HEPES solution (25 mM KCl, 2.5 mM $MgSO_4$, 1 mM DTT, 10 mM HEPES, pH 7.5). The resuspended axonemes were washed with HEPES solution by centrifugation (12,000 *g* for 20 min) and resuspended again in HEPES solution with or without 1 mM ATP and 100 μM sodium orthovanadate (final pH 7.5). About 5 min after resuspension, the axonemes were centrifuged at 27,000 *g* for 40 min, and the pellet was immediately frozen using a rapid-freezing apparatus.

Rapid-freezing and Replication: The rapid freezing method used in this study has been previously described in detail (11, 12). The axonemal pellet (with or without 1 mM ATP and 100 μM vanadate) was mounted on wet filter papers placed on a specimen holder and frozen by slamming the pellet against a pure copper block cooled to 4°K by liquid helium, using a newly developed freezing apparatus (16) (RF-10, Eiko Engineering, Mito, Japan). In some experiments, after mounting the pellet (without ATP and vanadate) on the specimen holder, a drop of 1 mM ATP in HEPES solution containing 0.1 mM EDTA was added to the pellet and allowed to sit for 5 s at room temperature. At the end of this incubation, the drop was quickly drained, and the pellet was rapidly frozen within 15 s. These frozen samples were stored in liquid nitrogen.

For deep-etching and replication, the frozen samples were brought directly into a conventional freeze-fracture apparatus (FD-3, Eiko Engineering, Mito, Japan) and, without fracturing, the metal-contacted surface of the samples was deeply etched *in vacuo* at 2×10^{-7} mm Hg followed by rotary shadowing (0.5 rps) with platinum (25°) and carbon (90°). The sample was then removed from the apparatus, treated with absolute methanol for 2–10 h, and immersed in household bleach (sodium hypochloride). The replicas that floated off the tissues were washed with distilled water and picked up on Formvar-filmed grids. The replicas were examined in a Hitachi 11-DS electron microscope at an accelerating voltage of 75 kV. Electron micrograph negatives were routinely contact-reversed and then printed as negative images. During all procedures, from picking-up of replicas to printing of photographs, careful attention was paid not to make mirror images of the real structures of axonemes.

ATPase Assay and Turbidity Measurement: To evaluate the activity of isolated axonemes, ATPase assays and turbidity measurements were made. The ATPase assay was performed in a reaction medium containing 1.0 mM ATP and 0.1 mM EDTA in HEPES solution (final pH 7.5), 20°C, at an axonemal protein concentration of 0.6 mg/ml. The reaction was initiated by the addition of ATP and terminated by adding trichloroacetic acid to a final concentration of 8% (wt/vol). Liberated inorganic phosphate was determined by a procedure modified from the method of Berenblum and Chain (17). The ATPase activity of axonemes was also assayed in the presence of 1 μM, 10 μM, 100 μM, and 1 mM sodium orthovanadate.

The axoneme disintegration induced by 1 mM ATP was monitored by measuring changes in the turbidity of an axoneme suspension (0.6 mg/ml in HEPES solution containing 0.1 mM EDTA) at 20°C, using a Hitachi 220 spectrophotometer. The effects of vanadate on the turbidity change were also measured.

The protein concentration was determined by the method of Lowry et al. (18).

RESULTS

Effects of ATP and Vanadate on Isolated Axonemes

The treatment of isolated cilia with 0.5% Triton X-100 removed the plasmalemma, resulting in naked axonemes accessible to exogenous substances such as ATP and vanadate. Such axonemes showed the typical 9 + 2 microtubule structure, essentially the same as that of intact cilia, in thin-section electron microscopy. We also confirmed in negative staining that, without any additional protease treatment, the axonemes underwent active sliding disintegration into individual doublets and groups of a few doublets following the addition of 1 mM ATP, as previously reported (6, 7). However, 100 μM vanadate completely inhibited such ATP-induced disintegration (data not shown). This effect was also detected spectrophotometrically; the ATP-induced turbidity change of the axonemal suspension at 350 nm became smaller as the concentration of vanadate increased. This inhibition reached a maximum of ~90% at the vanadate concentration of 100 μM and did not increase at all higher concentrations (Fig. 1). A similar dose-dependent relationship was obtained between the vanadate concentration and the ATPase activity of isolated axonemes; vanadate caused almost complete inhibition of axonemal ATPase activity at 100 μM (Fig. 1).

Since vanadate was reported not to interfere with the ATP-induced detachment of the dynein arms from the B-tubule but to inhibit their reattachment (5, 13, 19), we expected to recognize two distinct conformational states of dynein arms when isolated axonemes were treated with the two different HEPES solutions, (*a*) without ATP and (*b*) with 1 mM ATP and 100 μM vanadate.

Two States of Outer Dynein Arms

Since the frozen samples were not fractured, the freeze-etch replicas revealed the clear images of the lateral surface of axonemes in the holes of the outermost film that was artifactually produced on the air-liquid interface (Fig. 2). These holes were probably formed by peeling off or rupture of the outermost film, exposing the underlying axonemes. In the replicas, the lateral view of each axoneme showed 3–4 rods longitudinally oriented and 3–4 rows of globular structures between the rods. To interpret these lateral-view images, 0.5 M KCl-extracted axonemes, in which outer dynein arms were selectively removed, were examined by the same freeze-etch replica method. Such KCl-extracted axonemes were seen as 3–4 double rods free of globular structures (*inset* in Fig. 2). This was confirmed by thin-section electron microscopy. Furthermore, after ATP-induced disintegration of axonemes, each of the isolated doublets appeared to be one rod and one row of globular structures (data not shown). From these findings, it was concluded that the rods and globular structures seen in the lateral view of unextracted axonemes represent the B-tubules and the rows of outer dynein arms on the A-tubules, respec-

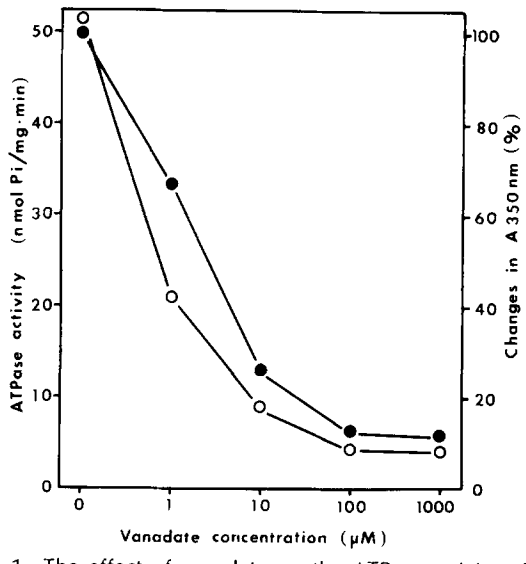

FIGURE 1 The effect of vanadate on the ATPase activity of axonemes (○) and the turbidity changes of an axonemal suspension (●). ATPase activity and turbidity changes were assayed in HEPES solution (25 mM KCl, 2.5 mM $MgSO_4$, 1 mM DTT, and 10 mM HEPES, pH 7.5) containing 1.0 mM ATP and 0.1 mM EDTA. Turbidity changes are shown as the percent decrease in absorbance at 350 nm caused by the ATP-induced disintegration of axonemes. Both ATPase activity and the turbidity changes are almost completely inhibited at the vanadate concentration of 100 μM.

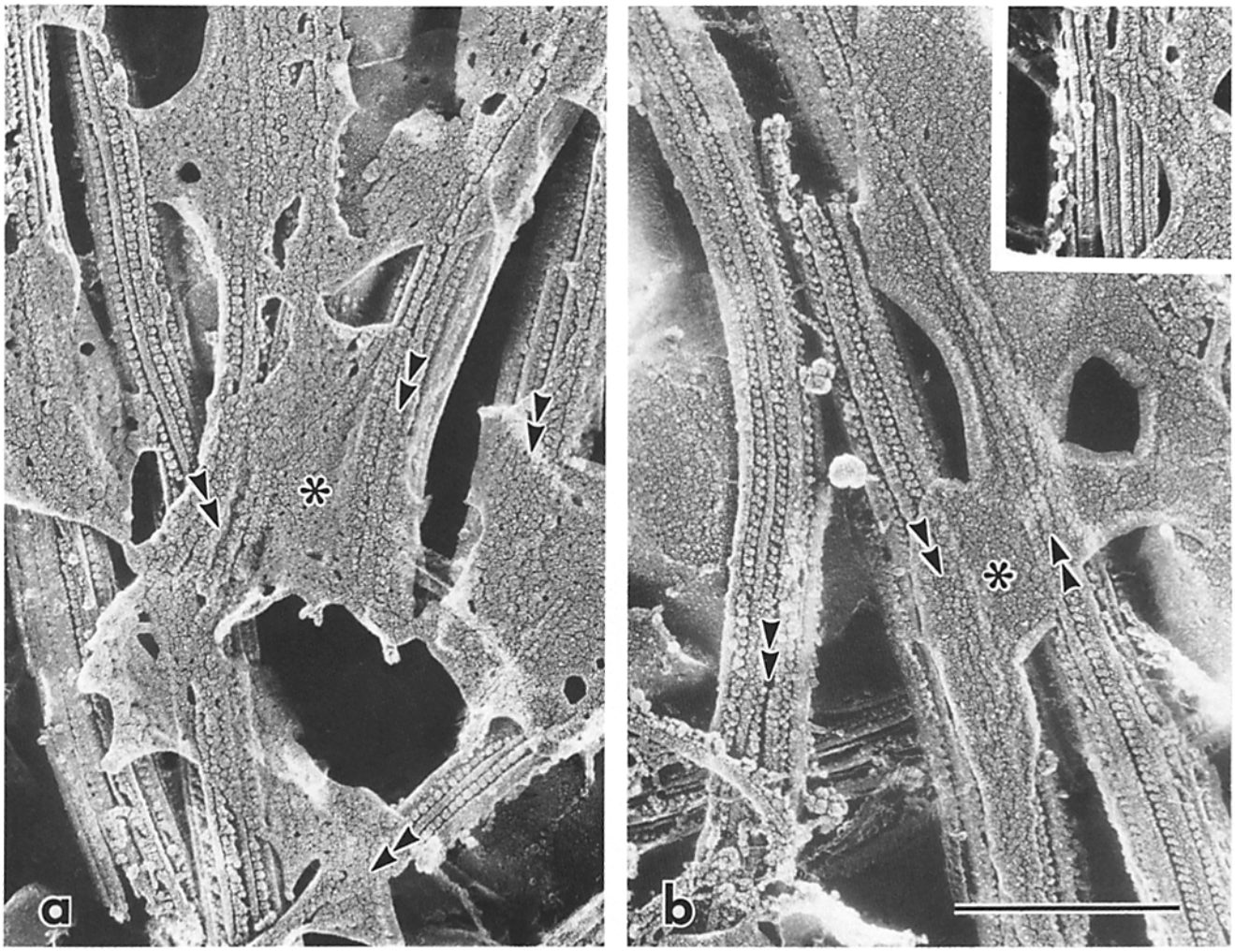

FIGURE 2 Electron micrographs of freeze-etch replicas of the metal-contacted surface of the axonemal pellet. The lateral views of axonemes are seen in the holes of the outermost film (*) which is artifactually produced on the air-liquid interface. Double arrowheads represent the baseward polarity of axonemes. × 64,000. Bar, 0.5 μm. (*a*) Axonemes in the absence of ATP. The axonemes are characterized by structurally uniform outer dynein arms which are arranged in rows between doublet microtubules at almost right angles. (*b*) Axonemes in the presence of 1 mM ATP and 100 μM vanadate. The outer dynein arms show a prominent baseward tilt. Note the difference in the structural conformations of outer dynein arms between (*a*) and (*b*). *Inset:* 0.5 M KCl-extracted axonemes. Axonemes were treated with 0.5 M KCl in HEPES solution for 5 min at 4°C before freezing. All outer dynein arms are removed by this treatment, exposing the A-tubule.

tively, and that the A-tubules were hardly seen behind the rows of outer arms. Moreover, the globular structures showed a repeating interval of 220 Å, almost the same repeat as that of the dynein arms described by negative-staining electron microscopy (3). The polarity of axonemes was readily determined according to the earlier descriptions of the three-dimensional architecture of axonemes (3).

When the axonemes in the absence of ATP were compared with those in the presence of 1 mM ATP and 100 μM vanadate, significant differences were discerned in the tilting angle and the structure of the outer dynein arms under the two different conditions (Fig. 2). In the absence of ATP, all axonemes were characterized by structurally uniform outer dynein arms that were attached to the doublet microtubules at almost right angles. Although it was difficult to determine the exact tilting angle of the outer arms in replica images, the arms in a full lateral view showed a slightly baseward tilt with the mean inclination of 11.1° ± 3.4° SD from the perpendicular to the doublet (see Fig. 4). On the other hand, in the presence of 1 mM ATP and 100 μM vanadate, in ~80% of the isolated axonemes, all arms showed a characteristically baseward tilt with the mean inclination of 31.6° ± 4.9° SD from the perpendicular (see Fig. 4). About 10–20% of the axonemes exhibited a tilt similar to that seen in the absence of ATP. Interestingly enough, both types of arms never coexisted in a single axoneme. We consider that the 10–20% of axonemes with the perpendicular configuration had become insensitive to ATP for some reason. Therefore, the arms with an almost *perpendicular* position (11.1°) and with a *tilted* position (31.6°) are here tentatively designated as "P-type" and "T-type," respectively.

Observations at higher magnifications revealed that, in addition to the difference in inclination, a significant difference in the structure of outer dynein arms also occurred between the P-type and the T-type (Fig. 3). The arms of the P-type showed an egg-shaped configuration of 27.0 nm ± 2.5 nm SD in length along the axis of the arm and 20.5 nm ± 2.3 nm SD in width, while those of the T-type were more extended and slender, measured to be 32.7 nm ± 3.6 nm SD in length and 16.7 nm ± 2.3 nm SD in width (see Fig. 4). These dimensions of outer dynein arms may be overestimated, because ~2-nm-

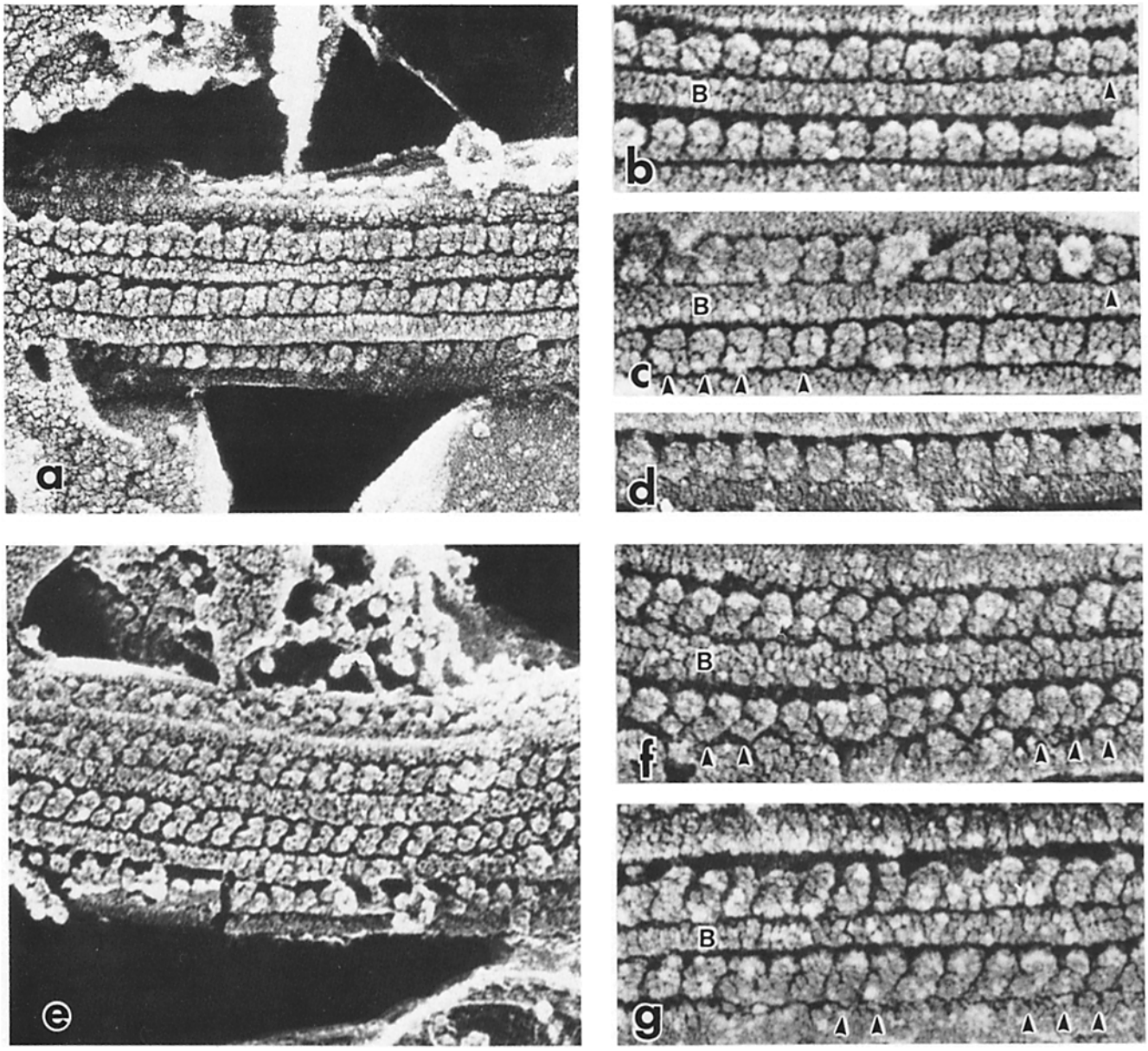

FIGURE 3 Comparison of the axonemes under two different conditions. In all micrographs, the base of each axoneme points to the right. In the absence of ATP (*a–d*), the axonemes possess the egg-shaped outer dynein arms which show a slightly baseward tilt with a mean inclination of 11.1° ± 3.4° SD from the perpendicular to the doublets (see Fig. 4). In the presence of 1 mM ATP and 100 μM vanadate (*e–g*), the arms are extended and slender and show a prominent baseward tilt with the mean inclination of 31.6° ± 4.9° SD from the perpendicular. Some outer arms (arrowheads) provided images of a possible subunit organization as shown in Fig. 4. Note the slender strands connecting each arm to an adjacent B-tubule in (*d*). B: B-tubule. *a* and *e*: × 173,000. *b–d*, *f* and *g*: × 264,000.

thick platinum was deposited in our specimens. Furthermore, the outer dynein arms provided images of a possible subunit organization as shown in Fig. 4. In particular, the T-type arms were seen to be composed of two spherical structures and a connecting rod. In both types of axonemes, some arms showed intermediate structural conformations and tilting angles between the P-type and the T-type (see Fig. 4 *b* and *c*). Interestingly, both arm types were occasionally seen with slender strands, each strand connecting an arm to an adjacent B-tubule (Fig. 3 *d*). Stereo pair electron microscopy showed that there were no detectable structural changes in either type of arm radially around the axoneme. It was difficult to measure precisely the interdoublet distance in the replicas.

Outer Dynein Arms in Reactivated Axonemes

The freeze-etch replica method was also used to examine whether the structural changes of outer dynein arms observed in P-type and T-type also occurred in ATP-reactivated axonemes. There were some difficulties in this approach. First, it took at least 20 s for the whole procedure from the administration of ATP to freezing. Therefore, at the time of freezing, most of the axonemes had completed their active sliding, and the replicas of the metal-contacted surface mainly contained disintegrated axonemes. Secondly, the possibility could not be excluded that some of the axonemes seen in replicas had not been directly exposed to ATP, because the incubation time

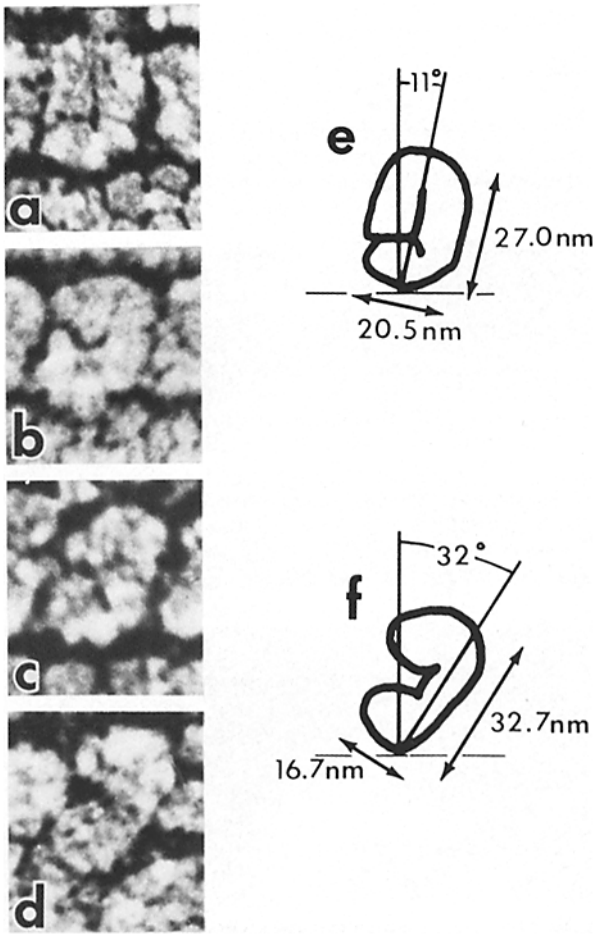

FIGURE 4 Structural conformations of outer dynein arms. Four lateral views of outer dynein arms are selected from the axonemes in the absence of ATP (*a* and *b*) and in the presence of 1 mM ATP and 100 μM vanadate (*c* and *d*). The arms in *a* and *d* are typical P- and T-type, respectively (see text for details), and those in *b* and *c* are intermediate-type arms. A possible subunit organization is seen in these arms. In *e* and *f*, average dimensions and inclinations of outer dynein arms of P- and T-type are shown, respectively. The standard deviation of each value is described in the text. The doublet microtubules to which the outer arms belong are on the lower side, and the base of the axonemes points to the right. × 640,000.

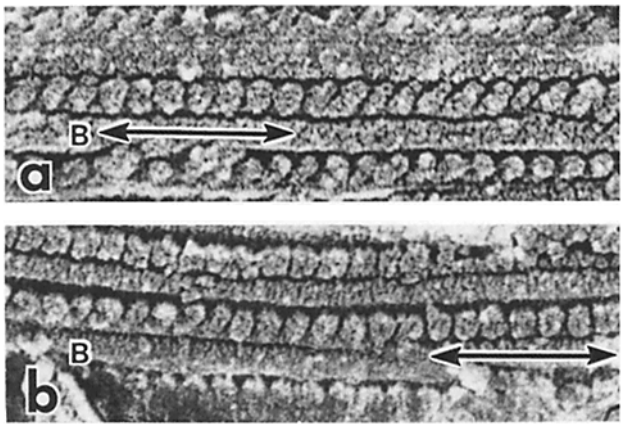

FIGURE 5 The lateral view of axonemes after administration of 1 mM ATP. The non- or partially disintegrated axonemes show the coexistence of the P-type (*arrows*) and T-type of outer dynein arms within one row of arms. Both types of arms are not mixed randomly, but tend to occur as groups along one row of arms. The base of the axonemes points to the right. *B:* B-tubule. × 173,000.

with ATP was very short (5 s). Nevertheless, in such ATP-treated axonemal samples, we could observe some significant features of the outer dynein arms between doublet microtubules in the nondisintegrated or partially disintegrated axonemes. Such reactivated axonemes often showed the coexistence of the P-type and T-type of outer arms within one row of arms (Fig. 5), which was not observed in the static axonemes incubated in the absence of ATP or in the presence of ATP and vanadate. Furthermore, both types of arms were not mixed randomly, but tended to occur as groups along one row of outer arms.

DISCUSSION

Taking advantage of the application of the rapid-freeze, deep-etch replica technique to the isolated axonemes from *Tetrahymena*, we have been able to demonstrate structural differences in outer dynein arms under two different conditions, i.e., in the absence of ATP and in the presence of ATP and vanadate. In the absence of ATP, the outer arms were oriented almost perpendicular to the doublets with a 11° baseward tilt, essentially consistent with the results obtained from the chemically fixed, thin-sectioned preparations of Satir et al. (4). Judging from available evidence, it is safe to say that such P-type arms occur in a "rigor" state, although in lateral-view replicas it is difficult to determine whether the doublets are really cross-bridged by the arms. On the other hand, in the presence of 1 mM ATP and 100 μM vanadate, the outer arms were characterized by a uniform, 32° baseward tilt, which was consistent with the negative-staining observations of isolated doublets (6, 7, 8). Both the axonemal ATPase activity and the ATP-induced turbidity changes of axonemal suspensions were almost completely inhibited by 100 μM vanadate. The combination of vanadate and ATP was reported to be a reliable and convenient condition for maintaining flagella in a relaxed state (5, 19). Hence, the T-type of arms can be regarded to occur in a "relaxed" state.

This paper is the first demonstration using nondisintegrated axonemes without any chemical fixation that the outer dynein arms occur in two distinct types of conformation, P- and T-types. In the replica images, the dynein arms appeared to have a subunit organization. As shown in Fig. 4, the outer arms are composed of three portions: a spherical part associated with the A-tubule ("body"), a spherical part in proximity to the adjacent B-tubule ("head"), and a connecting part ("neck"). In the P-type arm, the structure appears to be folded, making the "head" and "body" portions come close to show an egg-shaped outline. On the other hand, the T-type arm showed an extended configuration with three portions aligned in C-shape. Interestingly, arms of intermediate type were occasionally observed. The present results may explain the discrepancy between two previous observations on the subunit organization of isolated dynein arms, i.e., the linear arrays of three subunits observed by Warner et al. (20) and heart-shaped structures with two heads seen by Yano and Miki-Noumura (21). These two images are very similar to those of T- and P-type arms in our replica observations, respectively. It is still premature to discuss the sliding mechanism at the level of dynein subunits, but the present observations strongly suggest that the interdoublet sliding is caused by a dynamic conformational change of dynein arms, mainly by folding of the arm structures, which follows the hydrolysis of ATP (Fig. 6).

Our observations on the ATP-activated axonemes indicated that P- and T-type arms could coexist, often forming groups along one row of dynein arms. This suggests that the dynein

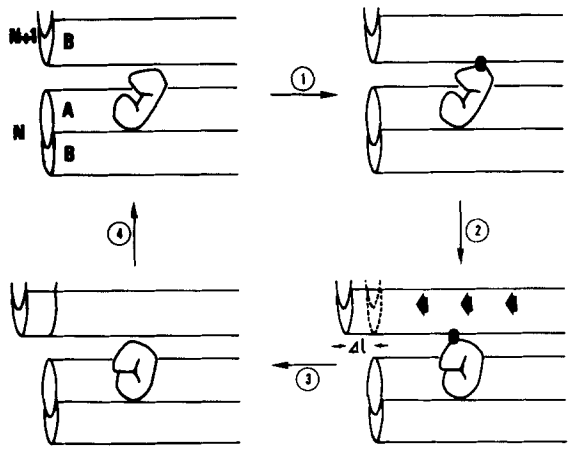

FIGURE 6 Postulated dynein cross-bridge cycle which is based on present observations and the models previously proposed by Satir et al. (4) and Sale and Gibbons (5). In the upper two states, the arm is the T-type, and in the lower two states, the P-type. As shown in Fig. 4, the T-type arm shows an extended configuration with three portions: a spherical part associated with the A-tubule ("body"), a spherical part in proximity to the adjacent B-tubule ("head"), and a connecting part ("neck"). The P-type arm appears to be folded, showing an egg-shaped outline. The following processes are considered in this model: Step *1*, attachment of the "head" portion of the arm to the adjacent B-tubule; Step *2*, interdoublet sliding caused by the structural change of the arm from T- to P-type; Step *3*, detachment of the "head" portion from the adjacent B-tubule; and Step *4*, structural change of the arm from P- to T-type. This model may be an oversimplification of the structural changes, since a possible rotation of the arm around its axis is neglected here. Probably, ATP-binding and ATP-hydrolysis occur in Steps *3* and *4*, respectively, and vanadate inhibits Step *1*. *A*, A-tubule; *B*, B-tubule; *N*, number of the doublet; Δl, sliding caused by one cycle of dynein arm.

arms may move in a nonrandom and cooperative manner. Indeed, the rapid-freeze, deep-etch replica technique used in this study is a powerful tool for in situ morphological analysis of the mechanochemical activities of the dynein arms, since this technique has good "temporal resolution" (9). However, before fruitful examination of such dynamic activities, we must determine how to control the time course of ATP incubation with greater precision and to raise the reactivation rate of the axonemes up to almost 100%. Information on the inner arm is also needed for a better understanding of ciliary movement. Studies along this line with the freeze-replica technique are currently being conducted in our laboratory.

We wish to thank Professor E. Yamada and Professor A. Yamauchi, Department of Anatomy, University of Tokyo, and Dr. M. Yano, Faculty of Pharmaceutical Science, University of Tokyo, for their valuable discussions and encouragement throughout this study. Special thanks are due to Professor H. Sakai, Department of Biophysics and Biochemistry, University of Tokyo, for his critical reading of this manuscript, to Dr. K. Kuroda, Department of Biology, Osaka University, for her kindly providing a stock culture of *Tetrahymena*, to Professor U. Sankawa and Dr. H. Noguchi, Faculty of Pharmaceutical Science, University of Tokyo, for letting us use the facilities for culturing *Tetrahymena*, and to Dr. M. E. Porter, Department of Biology, Ochanomizu University, for her critical reading of this manuscript. We also thank Mrs. M. Goto for her excellent technical assistance. Rapid freezing with liquid helium was carried out in the Cryogenic Center, University of Tokyo.

This study was supported in part by research grants from the Ministry of Education, Science and Culture, and from the National Center for Nervous, Mental, and Muscular Disorders of the Ministry of Health and Welfare, Japan.

Received for publication 14 July 1982, and in revised form 7 February 1983.

Note Added in Proof:—Similar results were obtained on the structural changes of the outer dynein arm in *Tetrahymena* cilia and *Chlamydomonas* flagella by U. W. Goodenough and J. E. Heuser (*J. Cell Biol.* 1982, 95:798–815). Recently, we have demonstrated that the outer dynein arm in *Tetrahymena* axonemes took a form of the P-type after the incubation with AMPPNP, a non-hydrolysable ATP analogue (S. Tsukita, S. Tsukita, and H. Ishikawa. 1983. *Biomedical Res.* In press).

REFERENCES

1. Satir, P. 1968. Studies on cilia. III. Further studies on the cilium tip and a "sliding filament" model of ciliary motility. *J. Cell Biol.* 39:77–94.
2. Summers, K. E., and I. R. Gibbons. 1971. Adenosine triphosphate-induced sliding of tubules in trypsin-treated flagella of sea urchin sperm. *Proc. Natl. Acad. Sci. USA.* 68:3092–3096.
3. Gibbons, I. R. 1981. Cilia and flagella of eukaryotes. *J. Cell Biol.* 91(No. 3, Pt. 2):107s–124s.
4. Satir, P., J. Wais-Steider, S. Lebduska, A. Nasr, and J. Avolio. 1981. The mechanochemical cycle of the dynein arm. *Cell Motility.* 1:303–327.
5. Sale, W. S., and I. R. Gibbons. 1979. Study of the mechanism of vanadate inhibition of the dynein cross-bridge cycle in sea urchin sperm flagella. *J. Cell Biol.* 82:291–298.
6. Sale, W. S., and P. Satir. 1977. Direction of active sliding of microtubules in *Tetrahymena* cilia. *Proc. Natl. Acad. Sci. USA.* 74:2045–2049.
7. Warner, F. D., and D. R. Mitchell. 1978. Structural conformation of ciliary dynein arms and the generation of sliding forces in *Tetrahymena* cilia. *J. Cell Biol.* 76:261–277.
8. Takahashi, M., and Y. Tonomura. 1978. Binding of 30S dynein with the B-tubule of the outer doublet of axonemes from *Tetrahymena puriformis* and adenosine triphosphate-induced dissociation of the complex. *J. Biochem.* 84:1339–1355.
9. Heuser, J. E., T. S. Reese, M. J. Dennis, Y. Jan, L. Jan, and L. Evans. 1979. Synaptic vesicle exocytosis captured by quick freezing and correlated with quantal transmitter release. *J. Cell Biol.* 81:275–300.
10. Heuser, J. E., and S. R. Salpeter. 1979. Organization of acetylcholine receptors in quick-frozen, deep-etch, and rotary-replicated *Torpedo* postsynaptic membrane. *J. Cell Biol.* 82:150–173.
11. Tsukita, S., S. Tsukita, J. Usukura, and H. Ishikawa. 1982. Myosin filaments in smooth muscle cells of the guinea pig taenia coli: a freeze-substitution study. *Eur. J. Cell Biol.* 28:195–201.
12. Tsukita, S., J. Usukura, S. Tsukita, and H. Ishikawa. 1982. The cytoskeleton in myelinated axons: a freeze-etch replica study. *Neuroscience.* 7:2135–2147.
13. Gibbons, I. R., M. P. Cosson, J. A. Evans, B. H. Gibbons, B. Houck, K. H. Martinson, W. S. Sale, and W.-J. Y. Tang. 1978. Potent inhibition of dynein adenosinetriphosphatase and of the motility of cilia and sperm flagella by vanadate. *Proc. Natl. Acad. Sci. U.S.A.* 75:2220–2224.
14. Watson, M. R., and J. M. Hopkins. 1962. Isolated cilia from *Tetrahymena pyriformis*. *Exp. Cell Res.* 28:280–295.
15. Gibbons, I. R. 1965. Chemical dissection of cilia. *Arch. Biol.* 76:317–352.
16. Usukura, J., E. Yamada, H. Akahori, and H. Takahashi. 1981. An improved device for rapid freezing using liquid helium. *J. Electron Microsc.* 30:214.
17. Berenblum, I., and E. Chain. 1938. An improved method for the colorimetric determination of phosphate. *Biochem. J.* 32:295–298.
18. Lowry, H., N. J. Rosebrough, A. L. Farr, and R. J. Randall. 1951. Protein measurement with the Folin phenol reagent. *J. Biol. Chem.* 193:265–275.
19. Okuno, M. 1980. Inhibition and relaxation of sea urchin sperm flagella by vanadate. *J. Cell Biol.* 85:712–725.
20. Warner, F. D., D. R. Mitchell, and C. R. Perkins. 1977. Structural conformation of the ciliary ATPase dynein. *J. Mol. Biol.* 114:367–384.
21. Yano, Y., and T. Miki-Noumura. 1981. Two-headed dynein arm. *Biomed. Res.* 2:73–78.